RESEARCH ARTICLE

INTERNATIONAL RESEARCH JOURNAL OF MULTIDISCIPLINARY TECHNOVATION

Asian Research Association

DOI: 10.54392/irjmt2463

Enhancing Paediatric Pneumonia Detection and Classification Using Customized CNNs and Transfer Learning Based Ensemble Models

Shubham Godbole [a,*], Adit Kattukaran [a], Saurin Savla [a], Vedant Pradhan [a], Pratik Kanani [a], Deepali Patil [a]

[a] Department of Artificial Intelligence (AI) and Data Science, Dwarkadas J. Sanghvi College of Engineering, Mumbai, India
* Corresponding Author Email: shubhamsgodbole@gmail.com
DOI: https://doi.org/10.54392/irjmt2463
Received: 18-07-2024; Revised: 19-10-2024; Accepted: 26-10-2024; Published: 30-10-2024

Abstract: Pneumonia is one of the most prominent causes of mortality in children who are below the age of five years in most parts of the globe. Hence, adequate pneumonia diagnosis is of paramount importance and is what drove this research effort which has led to the development of two transfer learning-based ensemble models. One of the proposed models classifies the chest radiographs into normal and pneumonia cases with outputs being generated from VGG-16, Inception-v3, and two custom-made convolutional neural networks, PneumoNet-v1 and PneumoNet-v2. The second model distinguishes bacterial from viral pneumonia with the help of Xception, MobileNet-v2, and PneumoNet-v1. To accomplish the aim of the study, the Guangzhou Women and Children's Medical Center dataset (Kermany Dataset) was used to benchmark model performance. PneumoNet-v1 and PneumoNet-v2 were designed with an emphasis for high classification accuracy and have individual accuracies of 96.2% and 96.8%, respectively for pneumonia detection. The first ensemble model used for classifying between healthy and infected images attained a classification accuracy of 98.03%. The second model used for differentiating between bacterial and viral demonstrated an accuracy of 91.93%. The effectiveness of transfer learning-based ensemble models as well as of the proposed custom CNN designs in enhancing the analysis of paediatric pneumonia and facilitating better diagnosis has been explored in this research.

Keywords: Transfer Learning, Weighted Ensemble, Paediatric Pneumonia, Customized CNN, Chest X-Rays (CXR)

1. Introduction

Pneumonia is an acute respiratory infection that inflames the lungs. Global health is severely impacted by this illness. Alveoli are small sacs which make up the lungs. When a healthy person breathes, they fill with air. The vital gas exchange within the alveoli is impaired by pneumonia. Pneumonia results in fluid filled alveoli and impairs oxygen exchange, filling alveoli with pus and fluid. This causes painful breathing and limits oxygen intake [1].

The severity of pneumonia depends on various factors like age, gender, state of health and the pathogen's type [2]. It causes an array of symptoms like cough, fever, shortness of breath, sweating and shaking chills, sharp pain in the chest which gets worse when we breathe or cough deeply. It is a severe lower respiratory tract infection with bacteria and viruses being the primary culprits though other pathogens can also be responsible including fungi [3]. This diversity in causative agents and the variable severity of the disease underscore the need for ongoing research. Understanding the coaction between host and pathogen, developing accurate diagnostics, and refining treatment strategies remain crucial for combating this significant global burden. Globally, pneumonia is a leading cause of morbidity and mortality in children younger than the age of 5 years [4]. According to the World Health Organization (WHO), globally 14% of all children below the age of 5 years succumb to pneumonia. This figure is nearly 700,000 per year or around 2000 every day. The impact of this disease is considerable worldwide, leading to significant healthcare expenses even in more developed regions. It can cause serious morbidity and require different treatment approaches, highlighting the importance of accurate diagnosis and classification.

Computed Tomography (CT), or as it is commonly called CT scan, is used for its high accuracy and detailed anatomical insights. It uses an amalgamation of radiographs and computer technology to produce detailed internal images of a body. It shows images of the bones, muscles, fat, organs and blood

vessels. However, due to concerns about radiation exposure and long-term health risks, chest radiographs are preferred for children [5]. Chest X-rays provide comparable sensitivity and greater specificity, making them suitable for accurate detection. Apart from the swift advancements in technologies such as bio-medical equipment, X-Rays have become increasingly cheaper. This research explores the use of chest radiographs for pneumonia diagnosis and aims to classify pneumonia into bacterial and viral types using various classification techniques.

Before the use of Artificial Intelligence (AI), doctors relied on physical signs like cough, fever, rapid breathing and abnormal lung sounds which they detected with the use of a stethoscope. Tapping the chest and listening to the sounds to identify the areas of fluid buildup in the lungs was also common practice. Later, chest X-rays became the primary tool to detect pneumonia. Deep learning techniques such as custom Convolution Neural Network (CNN) models have been widely trained on massive datasets of chest X-rays to help in faster analysis of the chest, improved accuracy and can learn subtle patterns in the X-rays missed by the human eye [6]. Soft computing methods such as Artificial Neural Networks (ANN), K-nearest neighbors (k-NN) and support vector machines (SVM) are also widely used for classification [7]. They also reduce the subjectivity of interpretation which helps in more consistent diagnosis across different radiologists.

This research delves into improving pneumonia diagnosis. This research delves into improving pneumonia diagnosis. The main contributions of this work are:

- Improving accuracy in detecting pneumonia with exceptionally high and consistent accuracy scores, especially for borderline cases. For this purpose, a weighted ensemble model combining the strengths of Inception-v3, VGG-16, PneumoNet-v1 and PneumoNet-v2 (two customized CNNs proposed in this research) has been employed.
- Existing research mainly focuses on binary classification between Normal and Pneumonia images. There is a need for an accurate model to further classify the type of Pneumonia into Viral or Bacterial for better diagnostics, for which another weighted ensemble model, amalgamating Xception, MobileNet-v2 and PneumoNet-v1 have been used.
- Development of two custom CNN architectures, PneumoNet-v1 and PneumoNet-v2 which efficiently extract the most relevant features from a Chest X-Ray Image for detecting pneumonia and further differentiating between viral and bacterial cases.

2. Related Works

2.1. Existing Methods

The ability of deep learning to detect pneumonia extends to its specific variant caused by COVID-19. Chowdhary *et al.* [8] proposed a technique for an automatic detection of COVID-19 pneumonia using pre-trained deep learning algorithms, achieving high detection accuracy of 97.9%. Similarly, Asnaoui *et al.* (2020) [9] conducted a comparative study of various deep learning models and found that Inception-ResNet-V2 (Accuracy = 92.18%) and DenseNet201 (Accuracy = 88.09%) provided the best results for the detection and classification of coronavirus pneumonia.

Deep learning models can go beyond binary classification (Pneumonia vs. Normal). Wang *et al.* [10] developed a CNN model using ResNet18 with a Visual Transformer. The CNN extracts spatial features from chest X-rays, while the Transformer determines the importance of each feature. Their model achieved an overall accuracy of 99.32% for Binary Classification between COVID-19 and non-pneumonia. However, the accuracy dropped considerably to 90.03% for four class classifications between COVID-19, Normal, Viral pneumonia and Bacterial pneumonia.

Ali *et al.* [11] investigated deep learning for pneumonia detection in paediatric patients. They implemented various Deep Convolutional Architectures for Binary Classification of Pneumonia between Normal and Pneumonia Images. They proposed an EfficientNetV2L model that achieved an accuracy of 94.02%. Their dataset included 5,863 images selected from retrospective cohorts of paediatric patients of one to five years old from Guangzhou Women and Children's Medical Centre, Guangzhou. Arulananth et al. (2024) [12] proposed a modified DenseNet121 Architecture where they introduced additional layers in the existing model. They introduced Batch Normalization, Max-Pooling and Drop out layers in model to improve its accuracy. All images were normalized using their mean and standard deviation to avoid overfitting. Only the training images underwent data augmentation. Their proposed architecture achieved an accuracy score of 97.03%, while classifying between Normal and Pneumonia images. Another such modified DenseNet architecture is mentioned in Sadik *et al.* [13] they have proposed a method to improve accuracy by parallel convolutions alongside the traditional model (DenseNet) for localization and efficient feature extraction. Their model achieved an accuracy of 87.5% while classifying among Pneumonia, COVID-19 and normal patients.

Deep learning research continues to explore strategies for improved performance in pneumonia detection. Hussain *et al*. [14] implemented a deep ensemble model using three pre-trained CNNs (VGG-16, DenseNet-201, and EfficientNet-B0) with transfer learning to extract deep features. Their dataset included

3,777 images in total. Equally split between COVID-19, Normal and Pneumonia Images (1,259 each). They further split these images in 70:30 ratio for training and testing dataset. Their ensemble model achieved an overall accuracy of 97% while classifying images into COVID19, Normal and Pneumonia (3 classes). [15] Loey et al. (2023) used a CNN and a Bayesian Optimizer for detecting COVID-19 pneumonia. CNN is used to extract features and Bayesian Optimizer adjusts the CNN hyper parameters based on an objective function.

While deep learning dominates the field, Rattan *et al.* (2024) [16] explored two approaches, the first using CNN-SVM (Support Vector Machine), CNN-LR (Logistic Regression) and CNN-KSVM (Kernel Support Vector Machine) and the second using CNN-RF (Random Forest), CNN-KNN (k-Nearest Neighbors), CNN-DT (Decision Tree), CNN-NB (Naïve Bayes). The CNN-SVM (Support Vector Machines) achieved the best accuracy of 95%. proposed a classification model that is constructed using fine-tuning a VGG16 architecture. Their dataset included 3,616 COVID-19, 1,345 pneumonia and 10,000 normal training images. This architecture achieved an accuracy of 95.79%.

Malik *et al.* (2023) [17] conducted a comprehensive study to build a deep convolutional neural network to classify 10 different chest diseases. Their two-step approach involves image segmentation followed by feature extraction. Information Maximizing GANs (Info-MGAN) is used initially on raw Chest X-rays (CXR) for image segmentation. This helps to create lung images of ten different chest diseases. For the next step, using Image processing techniques such as Speeded up Robust Features (SURF) and Oriented FAST and Rotated BRIEF (ORB) they extracted the discriminatory features to train the DCNNs. In the final step various CNN models are used to classify chest diseases. Overall, the literature highlights the growing interest and advancement of deep learning models for the detection of pneumonia, from Chest X-Rays (CXR), emphasizing the potential of these techniques in aiding in the diagnosis and classification of respiratory diseases.

These studies highlight the potential of deep learning not only for pneumonia detection but also for broader chest disease classification. Chouhan *et al.* [18] (2020) proposed a novel ensemble approach using transfer learning of five different pre-trained neural network architectures to classify pneumonia from chest X-ray (CXR) images. The ensemble model achieved an accuracy of 96.4% and on the Kermany dataset, outperforming previous state-of-the-art methods. The authors note that their approach can effectively detect the inflammatory region in chest X-ray (CXR) images of children, potentially improving the quality of pneumonia diagnosis and treatment.

Recent advancements in deep learning have shown promising results in automating pneumonia detection from X-rays, potentially aiding radiologists in diagnosis. One such approach is CheXNet, a 121-layer convolutional neural network developed by Rajpurkar *et al.* [19] Trained on the ChestX-ray14 dataset containing over 100,000 labelled chest X-rays, CheXNet achieved performance comparable to radiologists in identifying pneumonia.

Several studies have investigated transfer learning, where pre-trained models on large datasets are adapted for new tasks like pneumonia detection. Albahli *et al*. [20] explored InceptionResNet-V2 for this purpose, while Rahman *et al.* [21] investigated DenseNet-201. Similarly, Liang *et al*. [22] used ResNet-50 pre-trained on the ChestX-ray14 dataset itself, and Zubair *et al.* [23] opted for VGG-16. These approaches leverage the knowledge gained from large datasets to improve pneumonia detection accuracy.

While deep learning offers promising results, some studies explore alternative approaches. Chandra *et al.* [24] employed image processing techniques to segment lung regions in X-rays before classification. The features of region of interest (ROI) of the segmented lungs are extracted the method is examined on five benchmarks – Logistic Regression (LR), Sequential Minimal Optimization (SMO), Random Forest, Multilayer Perceptron (MP) and Classification via Regression.

The ability of building models using transfer learning quickly and reliably has helped many researchers build classifiers that can classify between Normal and Pneumonia patients. This technique allows for an ensemble model to work for a large dataset and generalize the results well. Hashmi *et al.* [25] implemented this strategy to develop an ensemble model by assigning weights to four different independent models – Xception, InceptionV3, DenseNet121 and MobileNetV3.

While deep learning dominates recent research, other techniques show promise for pneumonia detection in chest X-rays. Stephen *et al*. [26] explored a simpler approach using a seven-layer CNN model for X-ray image classification. This model demonstrates the ability of CNNs to automatically learn features for complex tasks like pneumonia detection. Zhang *et al.* [27] introduced a confidence-aware module for anomaly detection in lung X-rays. By framing pneumonia detection as a one-class classification problem (identifying anomalies like pneumonia), this approach can potentially improve model performance. Tuncer *et al.* [28] investigated applying fuzzy tree transformation to X-ray images. Exemplary division was then applied to these images followed by a multi kernel local binary pattern (MKLBP). The last step involves using iterative neighborhood component (INCA) to extract features. Interestingly, generating three different feature images improved the model's performance.

Jaiswal *et al.* [29] developed a mask region-based CNN for segmentation, followed by an ensemble

model for image thresholding. Their approach utilizes a threshold value in the background to improve model performance. Pan *et* al. [30] explored using an ensemble of Inception-ResNetv2, XceptionNet, and DenseNet-169 models for bounding box prediction. Ensemble learning allows the model to leverage the strengths of each model, potentially leading to increased accuracy in pneumonia localization.

Despite the critical health implications of both viral and bacterial pneumonia, there remains a significant lack of research focused on accurately distinguishing between these two types, especially through chest X-ray imaging. Nguyen *et al.* [31] addresses this gap by proposing a deep learning-based approach for differentiating viral and bacterial pneumonia. The authors developed a convolutional neural network (CNN) and employed explainability tools such as Local Interpretable Model-agnostic Explanations (LIME) and saliency maps to improve diagnostic accuracy. The method was tested on a dataset of chest X-ray images, with the CNN tasked with distinguishing between healthy individuals, viral pneumonia, and bacterial pneumonia. The model achieved a notable accuracy of 95.8% and an area under the curve (AUC) of 98.8% for classifying bacterial pneumonia versus normal images. However, accuracy was reduced when differentiating between bacterial and viral pneumonia, reaching 80.8% accuracy and an AUC of 88.8%, which was improved through the use of oversampling techniques to address data imbalance.

Nillmani *et al*. [32] addresses the limitations of conventional pneumonia classification systems, especially in distinguishing between viral, bacterial, and tubercular forms, including COVID-19. The authors propose a deep learning-based approach using seven pre-trained convolutional neural networks (CNNs) for multiclass classification of pneumonia using chest X-ray images. A total of 18,603 scans were used across binary, three-class, and five-class classification tasks. Among the models, DenseNet201 achieved the highest accuracy of 99.84% for binary classification (COVID-19 vs. other types of pneumonia), while VGG16 performed best for the three-class classification (COVID-19, Viral Pneumonia, and Normal) with an accuracy of 96.7%, and for the five-class classification (COVID-19, Viral Pneumonia, Bacterial Pneumonia, Tuberculosis, and Normal) with an accuracy of 92.7%. The study demonstrated that deep learning AI is a robust and efficient method for automatic pneumonia classification, outperforming existing methods by 1.2% in the five-class model.

2.2 Summary of Existing Methods

Table 1. Tabular Summarization of Existing Methodologies along with their Research Gaps and Results.

Literature	Approach	Research Gap	Results
Arulananth *et al.* [12]	Proposed a modified DenseNet101 with additional layers.	An overall simple architecture for classifying Normal and Pneumonia images but incapable of classifying among Viral and Bacterial Pneumonia.	Accuracy for two class classification – 97.03%.
Sadik *et al.* [13]	Performed parallel convolutions alongside DenseNet-121 architecture to find the region of interest.	An overall poor accuracy, unable to distinguish between Viral and Bacterial Pneumonia.	Accuracy for three class classification between Normal, COVID-19 and Pneumonia – 87.5%.
Rajpurkar *et al.* [19]	Developed a 121-layer CNN called CheXNet. Compared the performance of CheXNet to 4 practicing academic radiologists on a test set.	Due to training on 14 diseases, the results achieved for localizing and identifying Pneumonia are not satisfactory, Achieving an accuracy of just 76.80%.	Classifying 14 diseases results in mediocre accuracy levels for each disease.
Chandra *et al.* [24]	Used traditional computer vision and machine learning techniques to segment pixels that are most likely affected due to Pneumonia.	The limited number of images (412) restricts how well the findings can be applied to other datasets.	The Logistic Regression Classifier achieved an accuracy of 95.63% while Multilayer perceptron achieved 95.39%.

Hashmi *et al.* [27]	Ensemble Model - Xception, Inception-v3, DenseNet-121 and MobileNet-v3.	A large dataset and multiple models help generalize the model but couldn't further classify bacterial and viral pneumonia.	Heat maps show the affected regions in the lungs due to Pneumonia and their model achieved an accuracy of 98.4%.
Tuncer *et al.* [28]	Classification using Decision Trees and Support Vector Machines (SVM) and K-nearest neighbour (k-NN) methods. Data preparation step included Fuzzy tree transform to each image followed by exemplar division which is followed by a multi-kernel local binary pattern.	Very few data images cannot be generalised and an overall lengthy and time-consuming process for data preparation before applying classification algorithms.	Best accuracy was achieved by Cubic SVM – 97.01% for classifying between COVID-19, Pneumonia and Normal images.
Pan *et al.* [30]	Trained their models on a variety of image sizes which helped them identify that smaller sized images don't affect accuracy but also speed up the computation. An ensemble of Inception-ResNet-v2, XceptionNet, and DenseNet-169 to predict the bounding box and localise pneumonia affected regions.	Since most of their models were trained on positive images, the object detection models relied heavily on classification models to detect false positives.	Concatenated images of positive adjacent to a negative image helped identify false positives.

3. Methodology

3.1. Proposed Research

This work proposes two deep learning-based ensemble models: one for the classification of pneumonia and normal cases, another for differentiating between bacterial and viral pneumonia. The first ensemble model proposes a classification between pneumonia and normal cases by combining the output of four models: VGG-16, Inception-v3, PneumoNet-v1 and PneumoNet-v2 (two custom-built convolutional neural networks). The second ensemble model proposes differentiation between bacterial and viral pneumonia through the integration of the output provided by three models: Xception, MobileNet-v2, and PneumoNet-v1. The architectures and specifications of these models are provided along with a comparative analysis of existing models further in this research. Figure 1 illustrates the sequential steps involved in the proposed methodology.

3.2. Data Preprocessing

The chest radiographs (anterior-posterior) were collected from the publicly available Guangzhou Women and Children's Medical Center Dataset (Kermany dataset) which contains 5,856 X-ray images of paediatric pneumonia patients (from one to five years old) classified into a repository consisting of normal and pneumonia-affected cases. The dataset contains 1,583 radiographs for normal cases and 4,280 for pneumonia-affected cases. The pneumonia-affected cases from the Kermany dataset were divided into cases of bacterial and viral pneumonia, according to the labels given in the dataset. This resulted in 2,766 images for bacterial pneumonia and 1,514 images for viral pneumonia. Samples of CXR images present in the Kermany dataset have been shown in Figure 2. To address the scarcity of training data to classify the type of pneumonia, the dataset was increased using various data augmentation techniques such as horizontal flipping, random scaling, brightness/contrast adjustments, and shear transformations. All these methods were applied for improving dataset variability, model robustness, and hence generalize better on different imaging conditions. This approach increased the number of training samples for bacterial and viral pneumonia to 5,781 and 3,149 respectively, allowing for a diverse and vast dataset. Further, MobileNet-v2's preprocessing function was applied over these pixel values for normalization and standardization of image dimensions to 224×224 pixels which is the conventional input size for models pre-trained on the ImageNet dataset. The input dataset was then divided in the ratio 80:20 between the training set and test set, correspondingly.

3.3. PneumoNet-v1 Architecture

PneumoNet-v1, a novel customized CNN architecture for pneumonia detection, which also classifies the detected images into bacterial and viral pneumonia sub-classes, was developed. As shown in Figure 3, it has an input layer that is designed to accept images of size 224×224×3, relating to the height, width, and number of color channels of the input images respectively. The model architecture begins with a two-dimensional convolutional layer consisting of 128 filters of size 8x8, employing a stride of 3, followed by a batch normalization layer to reduce internal covariance shift and allow the network to train efficiently.

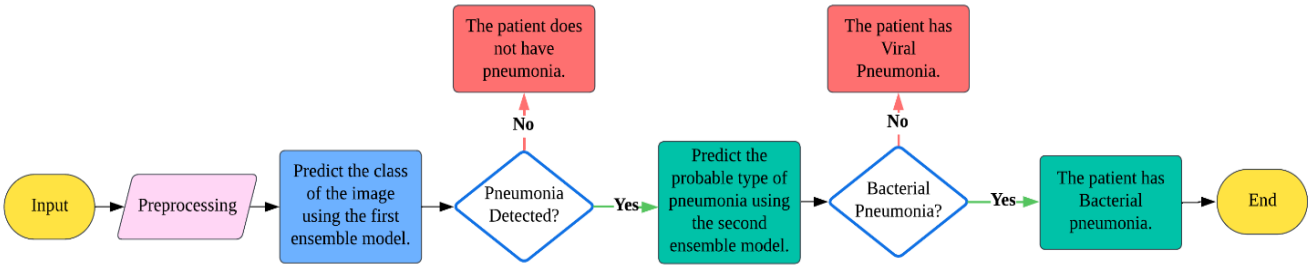

Figure 1. Methodology for Pneumonia detection and classification

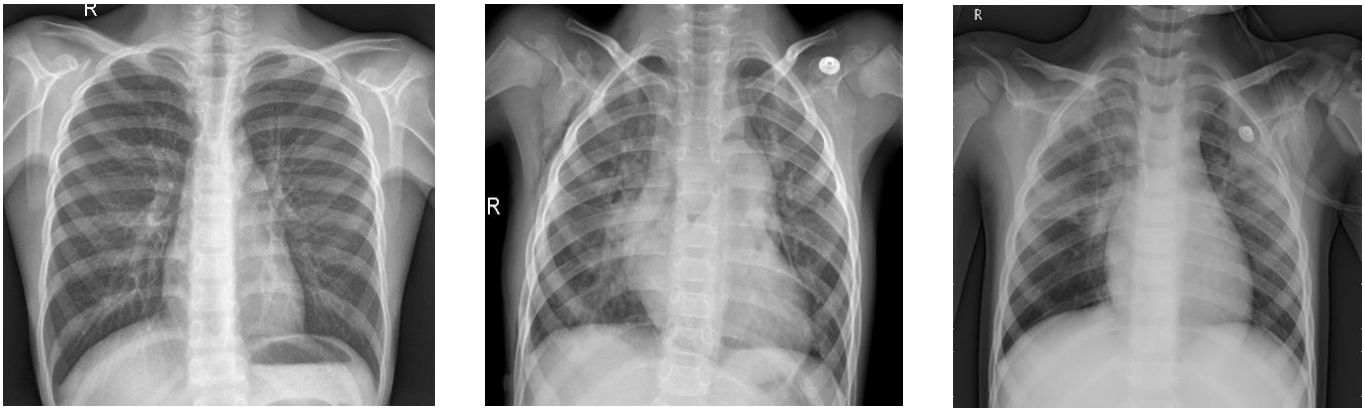

(a) (b) (c)

Figure 2. Radiographs from Kermany Dataset (a) Radiograph of a patient with healthy lungs (b) Radiograph of a bacterial pneumonia affected patient (c) Radiograph of a viral pneumonia affected patient.

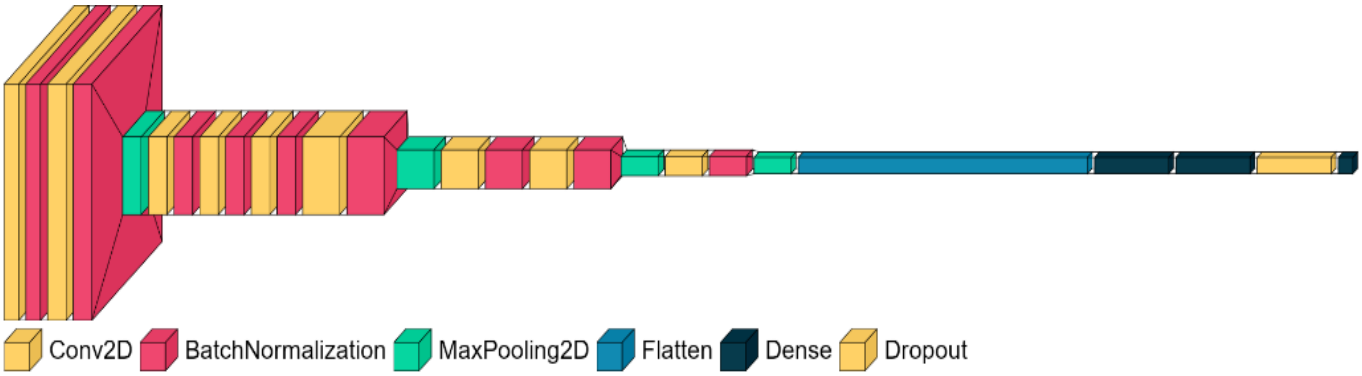

Figure 3. Architecture of proposed convolutional neural network PneumoNet-v1.

This step is succeeded by another convolutional layer with 256 filters of size 5x5 and a stride of 1, followed by batch normalization and a max pooling layer of size 3x3. In the subsequent three convolution layers, the first consists of 256 filters of size 3x3, while the other two have 256 filters each of size 1x1, with a stride of 1. Batch normalization is applied after each convolutional layer. Afterwards, four convolutional layers are enforced, each with 512 filters of size 3x3, succeeded by batch normalization and a max-pooling layer of size 2x2 after every convolution. The output from the final convolutional block is flattened into a one-dimensional array, which serves as the input to the dense layers, each containing 1024 units and ReLU activation functions in order to capture complex patterns. A dropout layer with an alpha value of 0.5 has been incorporated before the last dense layer to mitigate overfitting. The final layer is a dense layer with 2 units, corresponding to the two classes in the classification task, and utilizes a SoftMax activation function to produce the probability distribution over the classes. The model is compiled using Categorical Crossentropy as the loss function. For PneumoNet-v1, the learning rate was initialized at 10^{-4}, allowing a slow and steady learning process. The complete model architecture has been shown in Figure 3.

The stochastic gradient descent (SGD) was chosen as the optimizer to ensure a controlled convergence, better options for hyperparameter tuning and reduced chances of overfitting. SGD updates the parameters using the following formula:

$$\theta_{t+1} = \theta_t - \eta \nabla_\theta J\left(\theta_t; x^{(i)}, y^{(i)}\right) \quad (1)$$

$\theta_{t+1}\ and\ \theta_t$ represent the parameters at iterations t+1 and t respectively. $\nabla_\theta J\left(\theta_t; x^{(i)}, y^{(i)}\right)$ represents the gradient of loss function J with respect to parameters θ, evaluated at current parameters θ_t at ith training example $(x^{(i)}, y^{(i)})$. η represents the learning rate, a hyperparameter which determines the size of steps taken during the parameter update process. The parameters are updated using the computed gradient for each training example, scaled by the learning rate (shown in Eq. (1)). This process is repeated for each training example in the dataset, and this iterative process stops either when the parameters converge around values that minimize the loss function or until a pre-specified number of epochs is reached.

$$\theta_{t+1} = \theta_t - \eta \frac{1}{B} \sum_{i \in \mathcal{B}} \nabla_\theta J\left(\theta_t; x^{(i)}, y^{(i)}\right) \quad (2)$$

The Mini-Batch GD update rule adjusts the model parameters θ iteratively using gradients computed over mini-batches (batch size represented by B) of the training data (shown in Eq. (2)). This allows for parallelization and effective GPU utilization and leads to faster convergence compared to full batch gradient descent.

$$v_{t+1} = \gamma v_t + \eta \nabla_\theta J(\theta_t) \quad (3)$$

$$\theta_{t+1} = \theta_t - v_{t+1} \quad (4)$$

The Momentum Update rule modifies the parameter update step as shown in Eq. (3) and (4). $v_{t+1}\ and\ v_t$ represent the velocity terms as iterations *t*+1 and t respectively. The momentum coefficient is represented by γ , which controls the retention of previous velocity. γ helps accelerate the descent in the relevant direction and reduces its tendency to oscillate, enabling the optimizer to escape local minima more effectively.

3.4. PneumoNet-v2 Architecture

PneumoNet-v2, similar to PneumoNet-v1, is a customized CNN proposed in this research. It features a slightly different architecture (shown in Figure 4) compared to PneumoNet-v1. PneumoNet-v2 begins with an input layer of size 224x224x3, applying a two-dimensional convolutional layer with 64 filters and a 3x3 filter size, having a stride of 1, followed by a layer of batch normalization. Further, three convolutional layers, each having 128 filters, each of size 3x3 and a stride of 1. A batch normalization layer succeeds each convolution, and a 2x2 max pooling layer is applied after the first and third convolution. Afterwards, three convolution layers are applied, the first two having 256 filters and the third having 512, all having a filter size of 3x3, followed by a layer of batch normalization for each convolution. Max pooling with a 2x2 pool size is added after each layer. The output from the final convolution block is flattened into a one-dimensional array. This array is passed through two dense layers, having 1024 units each. Two dropout layers with a rate of 0.5 are applied after each dense layer to reduce overfitting. The architecture of the final dense layer is same as that of PneumoNet-v1. PneumoNet-v2 utilizes a lower learning rate during training and begins with a filter size of 64 instead of 128. These adjustments allow the model to extract intricate features which may have been overlooked by PneumoNet-v1. PneumoNet-v2 also uses the SGD optimizer like PneumoNet-v1, to achieve early convergence and allows for more hyper-parameter tuning alternatives.

3.5. Transfer Learning for Pneumonia Detection (Normal vs. Pneumonia)

A transfer learning approach with several pre-trained deep learning models was opted for accurate detection of pneumonia. This included models such as Xception, DenseNet-121, VGG-16, VGG-19, ResNet-50, MobileNet-v2, and Inception-v3. This methodology utilizes the features learned by these models and aims at enhancing the accuracy of the classification task. All models were trained on the Kermany dataset, and their test accuracies are reported in Table 2.

3.5.1. VGG-16

VGG-16 utilizes a deep stack of small convolutional layers to progressively extract features from images, reducing their dimensions through max pooling layers to manage overfitting [33]. The extracted features are classified by fully connected layers at the network's end, enabling precise object identification within images.

3.5.2. Inception-v3

Inception-v3 revolutionized the process with its inception module that treated images on multiple parallel paths as sub-networks [34]. This architecture consists of dimensionality reduction using 1x1 convolutions, feature extraction using 3x3 convolutions, and capturing fine details of the local information by 5x5 convolutions, followed by max pooling to retain the important features. Inception-v3 learns features on different scales and hierarchies effectively, helping in the classification of objects within images with improved accuracy and efficiency.

3.5.3. DenseNet-121

DenseNet-121 uses a unique architecture where the convolutional layers have dense connections i.e., they receive all the input from the previous layer [35].

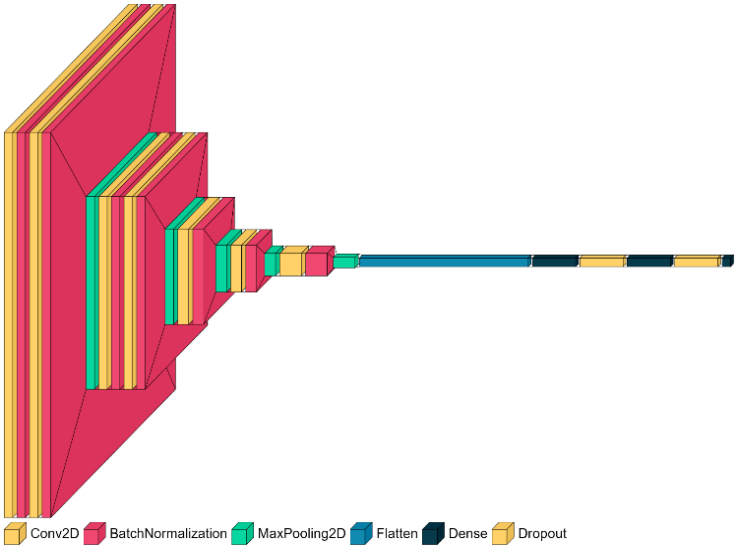

Figure 4. Architecture of proposed convolutional neural network PneumoNet-v2.

Table 2. Comparison of different tested algorithms for Pneumonia Detection (Normal vs. Pneumonia cases)

Model	Precision (Normal)	Precision (Pneumonia)	Recall (Normal)	Recall (Pneumonia)	F1-Score (Normal)	F1-Score (Pneumonia)	Validation Accuracy (%)	Test Accuracy (%)
VGG-16	0.95	0.95	0.88	0.98	0.91	0.97	94.2	95.1
VGG-19	0.93	0.94	0.88	0.95	0.90	0.95	93.0	92.9
Inception-v3	0.89	0.97	0.93	0.95	0.91	0.96	92.0	94.8
Xception	0.88	0.95	0.94	0.92	0.90	0.93	91.2	93.6
ResNet-50	0.81	0.92	0.81	0.92	0.81	0.92	88.5	89.0
DenseNet-121	0.98	0.95	0.88	0.99	0.92	0.97	96.5	95.8
Mobilenet-v2	0.96	0.97	0.93	0.99	0.94	0.98	96.4	96.8
PneumoNet-v1	0.97	0.96	0.89	0.99	0.93	0.97	96.1	96.2
PneumoNet-v2	0.96	0.97	0.93	0.99	0.94	0.98	96.2	96.8

This feature provides the highest information retention, and this type of connectivity reduces the vanishing gradient and leads to efficient parameter usage. These types of architectures are suitable for deep feature extraction.

MobileNet-v2, VGG-16, DenseNet-121, Inception-v3, PneumoNet-v1, and PneumoNet-v2 achieved the highest test accuracies (shown in Table 2) and hence these six models were shortlisted for the pneumonia detection task.

3.6. Transfer Learning for Pneumonia Classification (Bacterial vs. Viral)

A transfer learning approach with several pre-trained deep learning models was utilized to enhance classification performance for Pneumonia classification into bacterial and viral cases. These models included Xception, DenseNet-121, DenseNet-169, VGG-16, VGG-19, ResNet-50, ResNet-101, MobileNet-v2, and Inception-v3. All models were trained, and the test accuracy for each of them has been presented in Table 3.

3.6.1. Xception

Xception enhances the Inception architecture by integrating depth wise separable convolutions [36]. This approach splits the convolution operation into two layers: a depth wise convolution that filters each input channel independently, and a pointwise convolution that aggregates these filtered outputs through a 1x1 convolution. This structure reduces the number of parameters, making the network more efficient while potentially increasing performance. Xception's architecture includes a series of convolutional blocks designed to capture various levels of abstraction from

input images, facilitated by residual connections that enhance gradient flow and learning.

3.6.2. MobileNet-v2

MobileNet-v2 emphasizes on computational efficiency, introducing the inverted residual block, consisting of a 1x1 convolution to with ReLU followed by a 3x3 depth wise convolution for feature processing and finally another 1x1 convolution without non-linearity [37]. This configuration ensures efficient feature extraction while maintaining computational efficiency. MobileNet-v2 also employs linear bottlenecks, where the input and output dimensions are identical, facilitating efficient learning and feature extraction. Residual connections within the inverted residual blocks support better gradient flow during training, accommodating deeper networks. Xception, MobileNet-v2, PneumoNet-v1 and PneumoNet-v2 were the four models shortlisted for the bacterial vs. viral classification task, based on their test accuracies obtained in Table 3.

3.7. Ensemble Models

Numerous combinations of models were tested for pneumonia detection, with three, four, or five models in each ensemble, and finally a six model-ensemble approach. An unconventional meta-learning approach (specifically stacking) was also tested where a meta-learner model combines the predictions of base models, learning their prediction patterns to enhance overall accuracy. Accuracies of the five best performing ensembles along with the meta-learner model have been displayed in Table 4. Four combinations of three shortlisted models each were tested for Bacterial vs. Viral classification, along with an ensemble of all the shortlisted models and compared their accuracies as shown in Table 4, the top half being for pneumonia detection, and the bottom half being for pneumonia classification.

The exploration began with a straightforward approach that involved averaging the probability values for each class. This method resulted in a marginal improvement in accuracy over the pre-existing model but did not surpass the performance of the custom CNN models. Subsequently, a genetic algorithm was used to optimize the relative weights for each model's predictions within the ensemble. This approach led to a significant increase in accuracy. These methods also demonstrated similar improvements, all resulting in slightly higher accuracy. The most substantial improvement in performance was observed when a grid search was conducted for the weights over a search space ranging from 1 to 15. This process was repeated for each of the ensemble models which were combined using the models which had been shortlisted before. This allowed for exploration of a broad array of model weight ratios.

This approach yielded the highest overall accuracy and became the preferred optimization technique. Expanding the search space further resulted in diminishing returns and significantly increased computation time, as the process involved evaluating every possible combination. Using this chosen space of 15, the values for each possible combination of ensemble were calculated, after which the combination of Inception-v3, VGG-16, PneumoNet-v1 and PneumoNet-v2 was observed to be the best performing ensemble model for pneumonia detection.

Table 3. Comparison of different tested algorithms for Pneumonia Classification (Bacterial vs. Viral cases)

Model	Precision (Bacterial)	Precision (Viral)	Recall (Bacterial)	Recall (Viral)	F1-Score (Bacterial)	F1-Score (Viral)	Validation Accuracy (%)	Test Accuracy (%)
Xception	0.92	0.84	0.91	0.86	0.91	0.85	92.8	88.9
DenseNet-121	0.78	0.75	0.90	0.55	0.83	0.63	78.9	77.3
DenseNet-169	0.76	0.69	0.87	0.54	0.80	0.61	77.7	75.8
VGG-16	0.79	0.72	0.87	0.59	0.83	0.65	78.4	77.0
VGG-19	0.77	0.71	0.85	0.58	0.81	0.63	78.1	75.7
ResNet-50	0.78	0.68	0.89	0.63	0.82	0.61	82.0	79.4
ResNet-101	0.80	0.72	0.91	0.65	0.84	0.77	83.5	81.3
MobileNet-v2	0.84	0.83	0.92	0.69	0.88	0.75	87.2	83.7
Inception-v3	0.79	0.71	0.89	0.57	0.82	0.59	80.2	76.9
PneumoNet-v1	0.89	0.84	0.91	0.80	0.90	0.82	87.6	87.3
PneumoNet-v2	0.88	0.83	0.91	0.81	0.87	0.80	86.4	86.9

Table 4. Top performing models for pneumonia detection and classification

Combination (After calculating the optimal weights)	Test Accuracy (%)
Inception-v3, VGG-16, MobileNet-v2, PneumoNet-v1, PneumoNe2	97.5
DenseNet-121, MobileNet-v2, PneumoNet-v1, PneumoNet-v2	97.2
Inception-v3, VGG-16, PneumoNet-v1, PneumoNet-v2	98.0
DenseNet-121, VGG-16, MobileNet-v2, Inception-v3	96.2
MobileNet-v2, PneumoNet-v2, VGG-16, Inception-v3	97.6
Meta Learner (Inception-v3, VGG-16, PneumoNet-v1, PneumoNet-v2)	97.3
Xception, PneumoNet-v1, PneumoNet-v2	87.9
Xception, MobileNet-v2, PneumoNet-v2	87.3
Xception, PneumoNet-v1, MobileNet-v2	91.9
MobileNet-v2, PneumoNet-v1, PneumoNet-v2	84.2
Xception, MobileNet-v2, PneumoNet-v1, PneumoNet-v2	89.5
Meta Learner (Xception, PneumoNet-v1, MobileNet-v2)	89.7

The optimized relative weights were as follows: Inception-v3: 4, VGG-16: 5, PneumoNet-v2: 3, PneumoNet-v1: 1. the test accuracy calculated was 98.03%.

For the bacterial and viral classification, a similar approach was opted for. All the aforementioned techniques were applied, and it was noted that observed the most significant performance improvement was when a grid search for the weights within a range from 1 to 20 was conducted, beyond which the results were diminishing. Using this space, the values for each possible combination of ensemble were calculated, after which the combination of Xception, MobileNet-v2 and PneumoNet-v1 displayed the best results. The optimal weight values for Xception, MobileNet-v2 and PneumoNet-v1 were found to be 18, 9 and 8 respectively. The weighted ensemble model achieved a test accuracy of 91.93%.

4. Results

Sub-section 4.1 summarizes the results for Normal vs. Pneumonia cases (Pneumonia detection model), whereas sub-section 4.2 summarizes the results for the Bacterial vs. Viral classifications (Pneumonia classification model).

4.1. Evaluation of the Pneumonia Detection model (Normal vs. Pneumonia)

$$AUC = \int_0^1 (TPR) d(FPR) \quad (5)$$

Area under Curve (AUC) is a scalar ranging from 0 to 1, representing the model's overall performance. It is calculated using the formula in equation (5), where TPR represents the True Positive Rate and FPR represents the False Positive Rate. A high AUC indicates a strong model. The proposed weighted ensemble model for pneumonia detection achieved an AUC score of 0.97, indicating an extremely strong predictive ability. The Receiver Operating Characteristic (ROC) curve is a plot of the TPR and FPR on the y and x axes respectively. An area under curve value of 0.5 indicates no discriminative ability (random guessing) and a value of 1 indicates a perfect model. The ROC curve of the ensemble model and the models used in it are shown in Figure 5.

Figure 6 represents the confusion matrix for the Normal vs. Pneumonia classification. The precision for the Normal class was 0.97 and 0.98 for the Pneumonia class. The recall for the Normal class was 0.96 and 0.99 for the Pneumonia class. The F1-scores were calculated to be 0.97 and 0.99 respectively. The overall precision, recall and F1-score for the ensemble model was calculated to be 0.98. The final accuracy of the model after the ensemble was calculated to be 98.03%, which was significantly higher than Ali *et. al.* [11], Chouhan et al. [19], and most other published articles.

The model was also evaluated on the basis of Average Precision (AP) a metric used generally while dealing with imbalanced binary classification datasets. AP provides a single value summarizing the trade-off between precision and recall at different threshold values and is calculated using the following equation:

$$\text{AP} = \sum_n (R_n - R_{n-1}) P_n \quad (6)$$

As in equation (6), R_n is the recall in n^{th} threshold, and R_{n-1} is the recall in the $(n-1)^{th}$ threshold. P_n is the precision in the n^{th} threshold.

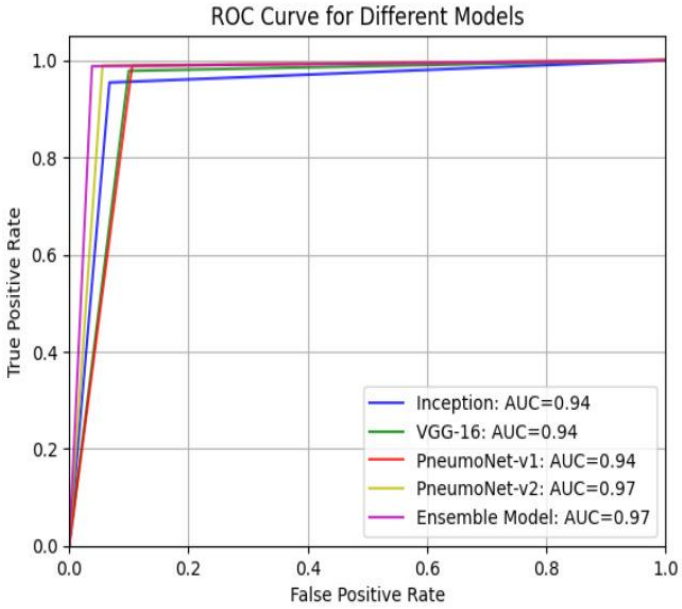

Figure 5. ROC curve for the ensemble model, Inception-v3, VGG-16, PneumoNet-v1 and PneumoNet-v2.

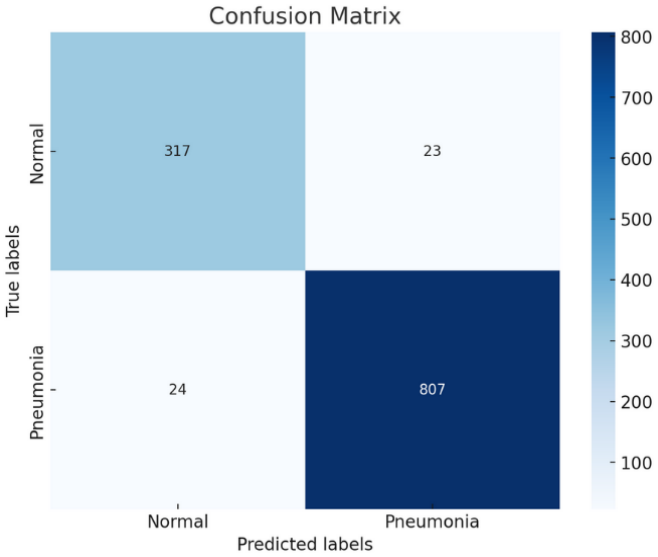

Figure 6. Confusion matrix for the ensemble model classifying normal and pneumonia patients.

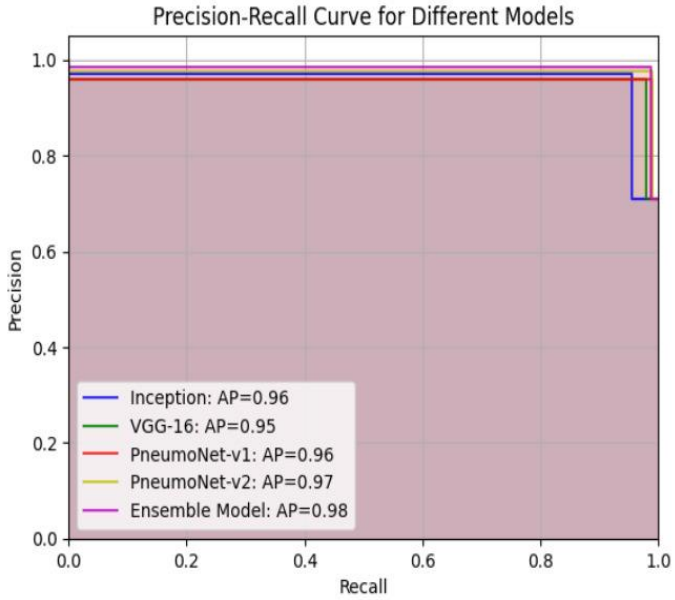

Figure 7. Precision-Recall curve for the ensemble model, Inception-v3, VGG-16, PneumoNet-v1 and PneumoNet-v2.

The value of AP calculated was 0.98 for the proposed model, indicating very strong ability to distinguish between normal and pneumonia classes. The Precision-Recall curve for the ensemble model as well as the models selected for the ensemble has been displayed in Figure 7.

4.2. Evaluation of the Pneumonia Classification model (Bacterial vs. Viral)

Figure 8. Represents the confusion matrix for the bacterial vs viral pneumonia classification. The precision for the bacterial class was 0.93 and 0.91 for the viral class. The recall for the bacterial class was 0.95 and 0.86 for the viral class. The F1-scores were calculated to be 0.94 and 0.88 respectively. The overall precision, recall and F1-score for the ensemble model was calculated to be 0.92. The final accuracy of the model after the ensemble was calculated to be 91.93%, surpassing all previous models.

The proposed ensemble model for classification of pneumonia into bacterial and viral achieved an AUC score of 0.91, indicating a strong predictive ability. The value of AP calculated was 0.83 for this model, indicating effective distinguishing between bacterial and viral classes, making it reliable in scenarios where both precision and recall are important. Figure 9 shows the ROC for the pneumonia classification model, and the Precision-Recall curve for the model has been shown in Figure 10.

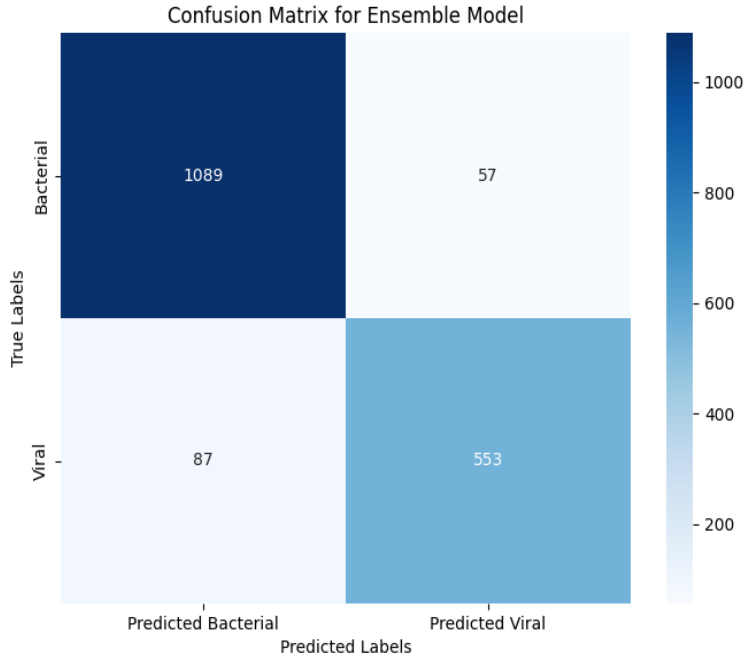

Figure 8. Confusion matrix for the ensemble model classifying bacterial and viral pneumonia.

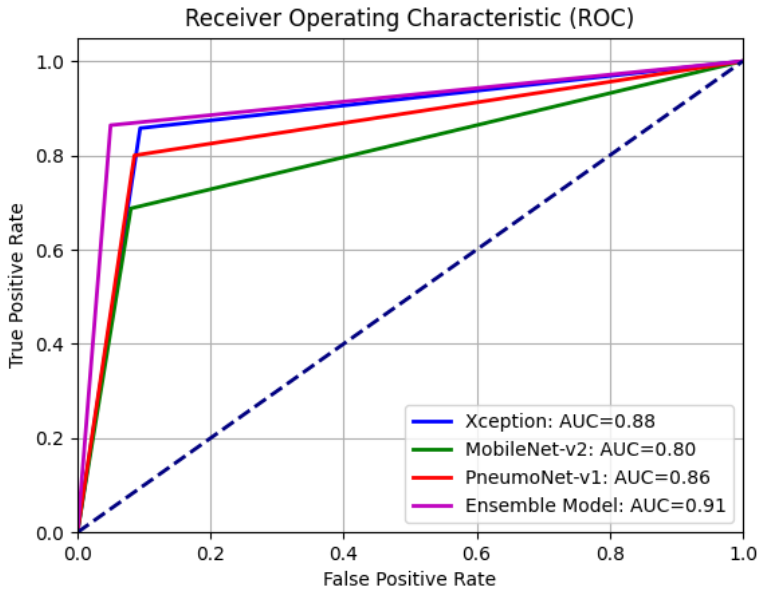

Figure 9. ROC curve for the ensemble model, Xception, MobileNet-v2 and PneumoNet-v1.

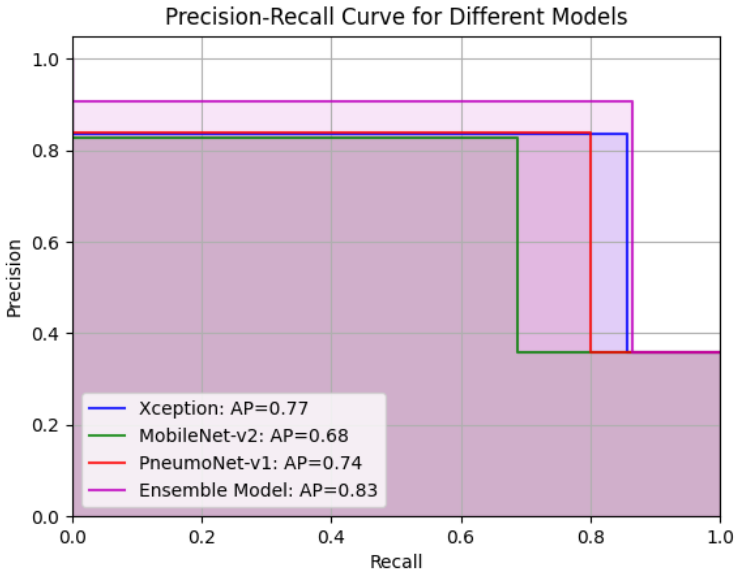

Figure 10. Precision-Recall curve for the ensemble model, Xception, MobileNet-v2 and PneumoNet-v1.

5. Conclusion

This research proposes two weighted ensemble models along with two customized convolutional neural network architectures, developed to improve the classification accuracy of paediatric pneumonia.

PneumoNet-v1 and PneumoNet-v2 are the proposed models which are specially designed CNN structures to successively classify the data. These two models significantly improved the accuracies of the ensemble models. PneumoNet-v1 displayed an individual accuracy of 96.2% for pneumonia detection and 87.3% for the classification into bacterial and viral pneumonia. PneumoNet-v2 achieved an individual accuracy of 96.8% for the Normal vs. Pneumonia classification.

The first weighted ensemble model is designed to classify pneumonia and normal cases using four algorithms: Inception-v3, VGG16, PneumoNet-v1, and PneumoNet-v2, resulting in an impressive classification accuracy of 98.03%, with a precision of 97.5% and a F1-score of 98%. The second weighted ensemble model focused on distinguishing between bacterial and viral pneumonia cases, utilizing a combination of Xception, PneumoNet-v1, and MobileNet-v2 achieving an accuracy of 91.93%. The overall precision and F1-score of the model is 91.89%.

Thus, the proposed ensemble models have proven to significantly increase the accuracy of the detection as well as the classification of paediatric pneumonia. However, the use of ensemble models results in increased computational inefficiency.

6. Future Scope

Pneumonia could be of multiple types, but the dataset used in this study had a limitation of only viral or bacterial cases. The curation of a new dataset from a reliable source consisting of multiple types of pneumonia could fill this research gap. Additional efforts could be made to synthetically generate and increase data using Generative Adversarial Networks (GANs). Multi-modal data integration could be done by combining radiographs with other data sources, such as patient history, lab results, etc. to improve detection accuracy and provide personalized diagnosis.

References

[1] C. Qin, D. Yao, Y. Shi, Z. Song, Computer-aided detection in chest radiography based on artificial intelligence: a survey. Biomedical engineering online, 17, (2018) 1-23. https://doi.org/10.1186/s12938-018-0544-y

[2] A. Sharma, D. Raju, S. Ranjan, (2017) Detection of pneumonia clouds in chest X-ray using image processing approach. In 2017 Nirma University International Conference on Engineering (NUiCONE), IEEE, India. https://doi.org/10.1109/NUICONE.2017.8325607

[3] B. Van Ginneken, B.T.H. Romeny, M.A. Viergever, Computer-aided diagnosis in chest radiography: a survey. IEEE Transactions on medical imaging, 20(12), (2001) 1228-1241. https://doi.org/10.1109/42.974918

[4] K. Kosasih, U. R. Abeyratne, V. Swarnkar, R. Triasih, Wavelet augmented cough analysis for rapid childhood pneumonia diagnosis. IEEE Transactions on biomedical engineering, 62(4), (2014) 1185-1194. https://doi.org/10.1109/TBME.2014.2381214

[5] H. Merzenich, L. Krille, G. Hammer, M. Kaiser, S. Yamashita, H. Zeeb, Paediatric CT scan usage and referrals of children to computed tomography in Germany-a cross-sectional survey of medical

practice and awareness of radiation related health risks among physicians. BMC Health Services Research, 12, (2012) 1-7. https://doi.org/10.1186/1472-6963-12-47

[6] Z. Ge, D. Mahapatra, X. Chang, Z. Chen, L. Chi, H. Lu, Improving multi-label chest X-ray disease diagnosis by exploiting disease and health labels dependencies. Multimedia Tools and Applications, 79, (2020) 14889-14902. https://doi.org/10.1007/s11042-019-08260-2

[7] S. Goyal, R. Singh, Detection and classification of lung diseases for pneumonia and Covid-19 using machine and deep learning techniques. Journal of Ambient Intelligence and Humanized Computing, 14(4), (2023) 3239-3259. https://doi.org/10.1007/s12652-021-03464-7

[8] M.E. Chowdhury, T. Rahman, A. Khandakar, R. Mazhar, M.A. Kadir, Z.B. Mahbub, K.R. Islam, M.S Khan, A. Iqbal, N.A. Emadi, M.B.I. Reaz, M.T. Islam, Can AI help in screening viral and COVID-19 pneumonia?. Ieee Access, 8, (2020) 132665-132676. https://doi.org/10.1109/ACCESS.2020.3010287

[9] K. El Asnaoui, Y. Chawki, Using X-ray images and deep learning for automated detection of coronavirus disease. Journal of Biomolecular Structure and Dynamics, 39(10), (2021) 3615-3626. https://doi.org/10.1080/07391102.2020.1767212

[10] T. Wang, Z. Nie, R. Wang, Q. Xu, H. Huang, H. Xu, F. Xie, X.J. Liu, PneuNet: deep learning for COVID-19 pneumonia diagnosis on chest X-ray image analysis using Vision Transformer. Medical & Biological Engineering & Computing, 61(6), (2023) 1395-1408. https://doi.org/10.1007/s11517-022-02746-2

[11] M. Ali, M. Shahroz, U. Akram, M.F. Mushtaq, S.C. Altamiranda, S.A. Obregon, I.D.L.T. Díez, I. Ashraf, Pneumonia Detection Using Chest Radiographs with Novel EfficientNetV2L Model. IEEE Access, 12, (2024) 34691 – 34707. https://doi.org/10.1109/ACCESS.2024.3372588

[12] T. S. Arulananth, S.W. Prakash, R.K. Ayyasamy, V.P. Kavitha, P.G. Kuppusamy, P. Chinnasamy, Classification of Paediatric Pneumonia Using Modified DenseNet-121 Deep-Learning Model. IEEE Access, 12, (2024) 35716 – 35727. https://doi.org/10.1109/ACCESS.2024.3371151

[13] F. Sadik, A.G. Dastider, M.R. Subah, T. Mahmud, S.A. Fattah, A dual-stage deep convolutional neural network for automatic diagnosis of COVID-19 and pneumonia from chest CT images. Computers in biology and medicine, 149, (2022) 105806. https://doi.org/10.1016/j.compbiomed.2022.105806

[14] A. Hussain, S.U. Amin, H. Lee, A. Khan, N.F. Khan, S. Seo, An automated chest X-ray image analysis for covid-19 and pneumonia diagnosis using deep ensemble strategy. IEEE Access, 11, (2023) 97207 – 97220. https://doi.org/10.1109/ACCESS.2023.3312533

[15] M. Loey, S. El-Sappagh, S. Mirjalili, Bayesian-based optimized deep learning model to detect COVID-19 patients using chest X-ray image data. Computers in Biology and Medicine, 142, (2022) 105213. https://doi.org/10.1016/j.compbiomed.2022.105213

[16] A. Rattan, Ritanshu, S. Singh, J. Pruthi, (2024) Comparative Analysis of Two Approaches Utilizing Different Classification Algorithms Combined with CNN for Pneumonia Prediction in Chest X-Rays. In 2024 14th International Conference on Cloud Computing, Data Science & Engineering (Confluence), IEEE, India. https://doi.org/10.1109/Confluence60223.2024.10463235

[17] H. Malik, T. Anees, M.U. Chaudhry, R. Gono, M. Jasiński, Z. Leonowicz, P. Bernat, A novel fusion model of hand-crafted features with deep convolutional neural networks for classification of several chest diseases using X-ray images. IEEE Access, 11, (2023) 39243-39268. https://doi.org/10.1109/ACCESS.2023.3267492

[18] V. Chouhan, S.K. Singh, A. Khamparia, D. Gupta, P. Tiwari, C. Moreira, R. Damaševičius, V.H.C. De Albuquerque, A novel transfer learning based approach for pneumonia detection in chest X-ray images. Applied Sciences, 10(2), (2020) 559. https://doi.org/10.3390/app10020559

[19] P. Rajpurkar, J. Irvin, K. Zhu, B. Yang, H. Mehta, T. Duan, D. Ding, A. Bagul, C. Langlotz, K. Shpanskaya, M.P. Lungren, A.Y. Ng (2017) Chexnet: Radiologist-level pneumonia detection on chest x-rays with deep learning. arXiv. https://doi.org/10.48550/arXiv.1711.05225

[20] S. Albahli, H.T. Rauf, A. Algosaibi, V.E. Balas, AI-driven deep CNN approach for multi-label pathology classification using chest X-Rays. PeerJ Computer Science, 7, (2021) e495. https://doi.org/10.7717/peerj-cs.495

[21] T. Rahman, M.E. Chowdhury, A. Khandakar, K.R. Islam, K.F. Islam, Z.B. Mahbub, M.A. Kadir, S. Kashem, Transfer learning with deep convolutional neural network (CNN) for pneumonia detection using chest X-ray. Applied Sciences, 10(9), (2020) 3233. https://doi.org/10.3390/app10093233

[22] G. Liang, L. Zheng, A transfer learning method with deep residual network for pediatric pneumonia diagnosis. Computer methods and programs in biomedicine, 187, (2020) 104964. https://doi.org/10.1016/j.cmpb.2019.06.023

[23] U. Shah, A. Abd-Alrazeq, T. Alam, M. Househ, Z. Shah, (2020) An efficient method to predict pneumonia from chest X-rays using deep learning approach. In The importance of health

informatics in public health during a pandemic, IOS Press, 457 – 460.

[24] T.B. Chandra, K. Verma, (2020) Pneumonia Detection on Chest X-Ray Using Machine Learning Paradigm. Proceedings of 3rd International Conference on Computer Vision and Image Processing. Advances in Intelligent Systems and Computing, Springer, Singapore.

[25] M.F. Hashmi, S. Katiyar, A.G. Keskar, N.D. Bokde, Z.W. Geem, Efficient pneumonia detection in chest xray images using deep transfer learning. Diagnostics, 10(6), (2020) 417. https://doi.org/10.3390/diagnostics10060417

[26] O. Stephen, M. Sain, U.J. Maduh, D.U. Jeong, An efficient deep learning approach to pneumonia classification in healthcare. Journal of healthcare engineering, 2019(1), (2019) 4180949. https://doi.org/10.3390/diagnostics10060417

[27] J. Zhang, Y. Xie, G. Pang, Z. Liao, J. Verjans, W. Li, W. Sun, J. He, Y. Li, Y. Xia, Viral pneumonia screening on chest X-rays using confidence-aware anomaly detection. IEEE transactions on medical imaging, 40(3), (2020) 879-890. https://doi.org/10.1109/TMI.2020.3040950

[28] T. Tuncer, F. Ozyurt, S. Dogan, A. Subasi, A novel Covid-19 and pneumonia classification method based on F-transform. Chemometrics and intelligent laboratory systems, 210, (2021)104256. https://doi.org/10.1016/j.chemolab.2021.104256

[29] A.K. Jaiswal, P. Tiwari, S. Kumar, D. Gupta, A. Khanna, J.J. Rodrigues, Identifying pneumonia in chest X-rays: A deep learning approach. Measurement, 145, (2019) 511-518. https://doi.org/10.1016/j.measurement.2019.05.076

[30] I. Pan, A. Cadrin-Chênevert, P.M. Cheng, Tackling the radiological society of North America pneumonia detection challenge. American Journal of Roentgenology, 213(3), (2019) 568-574. https://doi.org/10.2214/AJR.19.21512

[31] H.T. Nguyen, T. B. Tran, H.H. Luong, T.P. Le, N.C. Tran, Viral and bacterial pneumonia diagnosis via deep learning techniques and model explainability. International Journal of Advanced Computer Science and Applications, 11(7), (2020) 667-675. https://doi.org/10.14569/IJACSA.2020.0110780

[32] P.K. Nillmani, Jain, N. Sharma, M.K. Kalra, K. Viskovic, L. Saba, J.S. Suri, Four types of multiclass frameworks for pneumonia classification and its validation in X-ray scans using seven types of deep learning artificial intelligence models. Diagnostics, 12(3), (2022) 652. https://doi.org/10.3390/diagnostics12030652

[33] K. Simonyan, A. Zisserman, (2015) Very deep convolutional networks for large-scale image recognition. 3rd International Conference on Learning Representations (ICLR 2015), 1–14.

[34] C. Szegedy, V. Vanhoucke, S. Ioffe, J. Shlens, Z. Wojna, Rethinking the Inception Architecture for Computer Vision, IEEE Conference on Computer Vision and Pattern Recognition (CVPR), IEEE, USA. https://doi.org/10.1109/CVPR.2016.308

[35] G. Huang, Z. Liu, L. Van Der Maaten, K.Q. Weinberger, (2017) Densely Connected Convolutional Networks. IEEE Conference on Computer Vision and Pattern Recognition (CVPR), IEEE, USA. https://doi.org/10.1109/CVPR.2017.243

[36] F. Chollet, Xception: Deep learning with depthwise separable convolutions. In Proceedings of the IEEE conference on computer vision and pattern recognition, (2017) 1251-1258. https://doi.org/10.1109/CVPR.2017.195

[37] M. Sandler, A. Howard, M. Zhu, A. Zhmoginov, L. Chen, MobileNetV2: Inverted Residuals and Linear Bottlenecks. IEEE/CVF Conference on Computer Vision and Pattern Recognition, USA. https://doi.org/10.1109/CVPR.2018.00474

Authors Contribution Statement

Shubham Godbole: Conceptualization, Implementation, Methodology, Experimental Result Finding, Writing – Original Paper Drafting and Editing, Visualization, and Paper Formatting. Adit Kattukaran: Data Preprocessing, Implementation, Experimental Result Finding, Accuracy Assessment, Fine Tuning and Optimization. Saurin Savla: Conceptualization, Review of Existing Literatures, Writing - Paper Formatting, Editing, and Visualization. Vedant Pradhan: Introduction, Exploratory Data Analysis, Writing – Editing, Paper Formatting, and Proof Reading. Pratik Kanani: Supervision, Formal Analysis, Validation, Writing - Reviewing. Deepali Patil: Supervision and Validation. All the authors read and approved the final version of the manuscript.

Funding

The authors declare that no funds, grants or any other support were received during the preparation of this manuscript.

Competing Interests

The authors declare that there are no conflicts of interest regarding the publication of this manuscript.

Data Availability

The data supporting the findings of this study can be obtained from the corresponding author upon reasonable request.

Has this article screened for similarity?

Yes